5-1-1968

Surface Resonances In High Frequency Scattering From A Nearly-Sharp Three Dimensional Well.

Jaime Marcelo Wong Luy Tay

This thesis, directed and approved by the candidate's committee, has been accepted by the Graduate Committee of The University of New Mexico in partial fulfillment of the requirements for the degree of

Master of Science in Physics

SURFACE RESONANCES IN HIGH FREQUENCY SCATTERING FROM A NEARLY-SHARP THREE DIMENSIONAL WELL

Title

Jaime M. Wong L. T.

Candidate

Physics and Astronomy

Department

Arthur Stein

Dean

5-2-68

Date

Committee

Conf. Leavitt

Chairman

Seymour S Alpert

Derek B. Scarsar

SURFACE RESONANCES IN HIGH FREQUENCY SCATTERING FROM A NEARLY-SHARP THREE DIMENSIONAL WELL

By

Jaime M. Wong L.T.

A Thesis
Submitted in Partial Fulfillment of the
Requirements for the Degree of
Master of Science in Physics

The University of New Mexico
1968

ACKNOWLEDGMENTS

I would like to thank Dr. H. C. Bryant for suggesting this problem and also for his valuable advice in finishing it.

The author thanks Capt. Marion F. Schneider and Robert Conley for their advice and encouragement.

The valuable comments of Profesor C. Leavitt are also appreciated.

ABSTRACT

A computational investigation of the effect of a surface transition region of relative half-width δ on certain surface resonances in high frequencies scattering from a nearly-sharp, three dimensional spherical well is performed by the method of partial wave analysis.

An incident beam of particles, described by a scalar plane wave, interacts with a fixed scattering center represented by a dielectric sphere of index of refraction 1.333, with a very small transition region in the boundary of the well, described by an odd polynomial function of third order. This is the scalar-wave analogue to the more complicated problem of scattering of light from water droplets.

For the case of size parameter (propagation constant times the well radius) near 200, four different resonances were found, each of which has a period of about 0.81 in the size parameter X.

Plots of the size parameter at the resonances and the average probability density of finding the particle inside the well (excluding the transition zone) vs the half-width of the transition region, δ, were made and a linear dependence in each case was found for small values of δ.

Also, a plot of the width of the resonances (which are assumed to have a Lorentzian line shape behavior) vs δ was made and is shown to be related to the graph of the probability density vs δ.

The calculations demonstrate that the surface resonance excited by a monochromatic beam of particles in the resonance regions is due mainly to the terms in the partial wave expansion representing the highest contributing value of the angular momentum.

CONTENTS

LIST OF FIGURES

I. GENERALITIES

We wish to consider a scattering experiment in which a single fixed sphere is bombarded by a beam of particles represented by an incident plane wave. The potential energy of the particle in the neighborhood of the scattering center is defined to be a square well of radius a with a very small and smooth transition zone in the region $a-\delta/k \leq r \leq a+\delta/k$ (Figure 1).

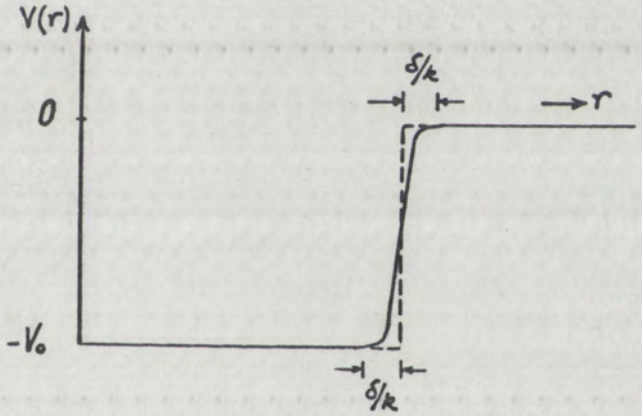

Figure 1. The dependence of the potential energy on radius.

The incident beam is described by a scalar plane wave traveling along the positive z direction,

$$u_{inc}(r, \theta) = e^{ikz} = e^{ikr\cos\theta},$$

which can be expanded in terms of partial waves in the standard way:[1]

$$u_{inc}(r,\theta) = \sum_{l=0}^{\infty} (2l+1)\, i^l j_l(kr) P_l(\cos\theta) , \qquad (2)$$

where $k = \left[2\mu E/\hbar^2\right]^{1/2}$. μ, E, k represent the mass, energy and the wave number of an incident beam particle respectively. The functions j_l (kr), P_l (cosθ) are the spherical Bessel functions and the Legendre polynomials, where the angular momentum quantum number is represented by l.

Throughout this paper, spherical polar coordinates are used with the angle θ measured from the positive z direction.

When the incident wave interacts with the spherical potential, a standing wave inside the well and an outward spherical wave outside the well are produced.
The outgoing scattered wave is expanded in terms of the spherical Hankel functions of the first class, $h_l^{(1)}$(kr), and the Legendre polynomials:[1]

$$u_{os}(r,\theta) = \sum_{l=0}^{\infty} A_l h_l^{(1)}(kr) P_l(\cos\theta) \qquad (3)$$

The A_l's are constant coefficients to be determined, and the Hankel functions are related to the spherical Bessel functions and the Neumann functions, n_l (kr), according to:

$$h_l^{(1)}(kr) = j_l(kr) + i n_l(kr) . \qquad (4)$$

The outgoing wave was chosen to have the form of a spherical

wave whose asymptotic behavior is given by

$$\lim_{kr\to\infty} h_\ell^{(1)}(kr) = \frac{1}{kr}\, e^{i\left(kr-(\ell+1)\frac{\pi}{2}\right)} . \qquad (5)$$

The wave function outside the well is a linear superposition of the incident particle wave function and the outgoing scattered wave:

$$u_{out}(r,\theta) = u_{os}(r,\theta) + u_{inc}(r,\theta) ,$$

$$u_{out}(r,\theta) = \sum_{\ell=0}^{\infty} A_\ell\, h_\ell^{(1)}(kr)\, P_\ell(\cos\theta) + \sum_{\ell=0}^{\infty} (2\ell+1)\, i^\ell\, j_\ell(kr)\, P_\ell(\cos\theta) . \qquad (6)$$

The wave inside the well has the form:

$$u_{ins}(r,\theta) = \sum_{\ell=0}^{\infty} C_\ell\, I_\ell(kr)\, P_\ell(\cos\theta) . \qquad (7)$$

The C_ℓ's are again constant coefficients that will be determined later.

The $I_\ell(kr)$ are functions that are solutions of the Schroedinger radial equation:

$$\frac{1}{r^2}\frac{\partial}{\partial r}\left(r^2\frac{\partial}{\partial r}R\right) + \left[\frac{2\mu}{\hbar^2}(E-V(r)) - \frac{\ell(\ell+1)}{r^2}\right] R = 0 ,$$

which can be written in the following way,

$$\frac{d^2R}{dr^2} + \frac{2}{r}\frac{dR}{dr} + \left[\frac{2\mu(E-V(r))}{\hbar^2} - \frac{\ell(\ell+1)}{r^2}\right] R = 0. \qquad (8)$$

The last equation can be written in terms of the index of refraction, which can be defined as follows:

$$m(r) = \left(\frac{E - V(r)}{E} \right)^{1/2} . \qquad (9)$$

Let $\rho = kr$ and write the Schroedinger equation in terms of ρ and the index of refraction $m(\rho)$:

$$\frac{d^2R}{d\rho^2} + \frac{2}{\rho}\frac{dR}{d\rho} + \left[m^2(\rho) - \frac{l(l+1)}{\rho^2} \right] R = 0 . \qquad (10)$$

The solution of this equation is identified with the spherical Bessel functions, $j_l(M\rho)$ in the region where the index of refraction is constant ($m(\rho) = M = 1.333$), namely for $r \leq a - \delta/k$, but as a linear combination of spherical Bessel functions, $j_l(\rho)$ and Neumann spherical functions, $n_l(\rho)$ for $r \geq a + \delta/k$.

We wish to consider a special case for the potential V(r) as follows:

An odd polynomial function of third order with center at (ka, A) is chosen for the index $m(\rho)$ in the interval $X - \delta \leq \rho \leq X + \delta$.

$$m(\rho) = A + B(\rho - X) + C(\rho - X)^3 \quad \text{for} \quad X - \delta \leq \rho \leq X + \delta ,$$

where A, B, C are constant coefficients and $X = ka = 2\pi a/\lambda$ represents the size parameter of the well. In terms of an optical model, a water droplet for instance, the size parameter is just the ratio of the circumference of the water droplet to the wavelength of the incident beam.

The cubic odd polynomial function was chosen in this way so that the derivative of the index of refraction with respect to the parameter ρ vanishes at $\rho = X - \delta,\ X + \delta$. This condition assures that the index of refraction is a continuous function and has a continuous first derivative.

The index of refraction can also be written as a function of the parameter ρ', where ρ' is measured from the size parameter X (Figure 2).

$$m(\rho') = A + B\rho' + C\rho'^3 \qquad (11)$$
$$\rho' = \rho - X$$

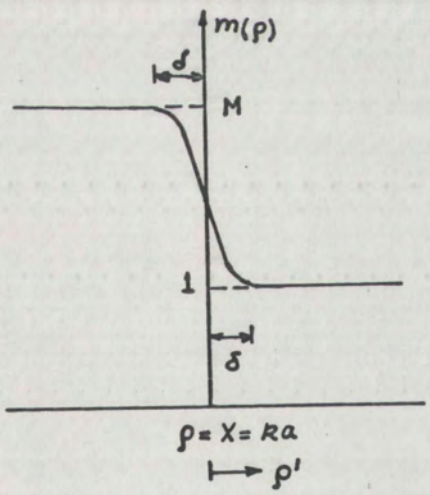

Figure 2.

The constant coefficients A, B, C can be determined according to the boundary conditions at $\rho' = \pm \delta$.

$$m(\rho)_{\rho'=-\delta} = M. \qquad (12a) \qquad \left.\frac{dm}{d\rho'}\right|_{\rho'=-\delta} = 0. \qquad (12c)$$

$$m(\rho)_{\rho'=+\delta} = 1. \qquad (12b) \qquad \left.\frac{dm}{d\rho'}\right|_{\rho'=+\delta} = 0. \qquad (12d)$$

Conditions (12c) and (12d) give the same equation at $\rho' = \pm \delta$, which together with eqs. (12a) and (12b) provide three independent equations to solve for A, B, C:

$$\begin{aligned} A &= (M+1)/2, \\ B &= 3(1-M)/(4\delta), \\ C &= -B/(3\delta^2). \end{aligned} \qquad (13)$$

Since the index of refraction is not constant in the transition zone of width 2δ, the use of numerical integration is required to evaluate eq.(10) subject to the boundary conditions at $\rho = X-\delta$.

$$I_\ell(\rho)\Big|_{\rho=X-\delta} = j_\ell[M(X-\delta)]. \qquad \ell = 0, 1, 2, \ldots \qquad (14)$$

$$I'_\ell(\rho)\Big|_{\rho=X-\delta} = j'_\ell[M(X-\delta)]. \qquad \ell = 0, 1, 2, \ldots \qquad (15)$$

where the prime denotes the derivative with respect to the parameter ρ, i.e.,

$$' = \frac{d}{d\rho}.$$

II. NUMERICAL INTEGRATION

The Runge-Kutta method and the Euler-Taylor expansion have been used to calculate the "special" spherical Bessel functions, $I_\ell(\rho)$, and their first derivatives $I'_\ell(\rho)$, starting at $\rho = X - \delta$ and integrating numerically through the transition region until $\rho = X+\delta$.

The special Bessel functions of higher angular momentum can be generated by means of the recursion relation[4] at $\rho = X-\delta$,

$$I_{\ell-1}(\rho) + I_{\ell+1}(\rho) = \frac{2\ell+1}{\rho} I_\ell(\rho) . \tag{16}$$

$$I'_\ell(\rho) = I_{\ell-1}(\rho) - \frac{\ell+1}{\rho} I_\ell(\rho) \tag{17}$$

These recursion relations are applied for $\ell \geq 2$ and require the knowledge of I_ℓ and I'_ℓ for $\ell = 0, 1$.

Thus,

$$I_0(\rho)\Big|_{\rho=X-\delta} = j_0[M(X-\delta)] = \frac{\sin M(X-\delta)}{M(X-\delta)} .$$

$$I_1(\rho)\Big|_{\rho=X-\delta} = j_1[M(X-\delta)] = \frac{\sin M(X-\delta)}{[M(X-\delta)]^2} - \frac{\cos M(X-\delta)}{M(X-\delta)} .$$

$$I'_0(\rho)\Big|_{\rho=X-\delta} = j'_0[M(X-\delta)] = M\left[\frac{\cos M(X-\delta)}{M(X-\delta)} - \frac{\sin M(X-\delta)}{[M(X-\delta)]^2}\right].$$

$$I'_1(\rho)\Big|_{\rho=X-\delta} = M\left[\frac{\sin M(X-\delta)}{M(X-\delta)} + \frac{2\cos M(X-\delta)}{[M(X-\delta)]^2} - \frac{2\sin M(X-\delta)}{[M(X-\delta)]^3}\right].$$

i) THE RUNGE-KUTTA METHOD [5,6]

The Runge-Kutta method is one of the most accurate methods used in solving numerically any differential equation of order n.

We can apply this method to solve numerically the radial Schroedinger differential equation given by eq. (10), which has the form $I'' = f(\rho, I, I)$. The initial condition is given at $(\rho_o, I(1))$ where $\rho_o = X-\delta$ for any ℓ.

The problem is to find the $I_\ell(2)$ corresponding to the new point $\rho = \rho_o + h$ (Figure 3). Once $I_\ell(2)$ is found, a new I_ℓ value, $I_\ell(3)$, can then be obtained that corresponds to a second value at $\rho_o + 2h$. In this way, the second order differential equation is integrated step by step and the required dependence of I_ℓ on ρ can be determined.

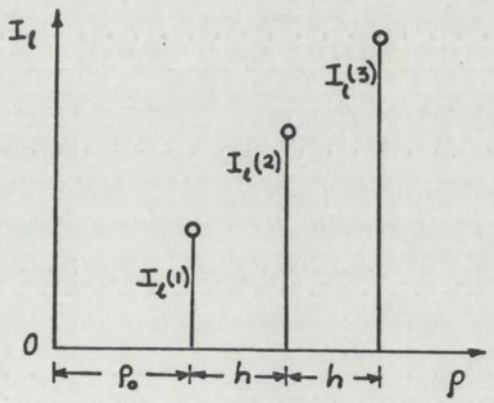

Figure 3. Illustration of the step by step integration of equation (10).

The basic formulas for the Runge - Kutta method are applied in the following order :

$$I_\ell(n+1) = I_\ell(n) + \Delta I_\ell(n), \tag{18}$$

$$I'_\ell(n+1) = I'_\ell(n) + \Delta I'_\ell(n). \tag{19}$$

$$\Delta I_\ell(n) = h\left[I'_\ell(n) + \frac{1}{6}(k_1+k_2+k_3)\right]. \tag{20}$$

$$\Delta I'_\ell(n) = \frac{1}{6}(k_1 + 2k_2 + 2k_3 + k_4). \tag{21}$$

$$k_1 = hf(\rho_n, I_\ell(n), I'_\ell(n)).$$

$$k_2 = hf\left(\rho_n+\frac{h}{2}, I_\ell(n)+\frac{h}{2}I'_\ell(n) + \frac{h}{8}k_1, I'_\ell(n)+\frac{k_1}{2}\right).$$

$$k_3 = hf\left(\rho_n+\frac{h}{2}, I_\ell(n)+\frac{h}{2}I'_\ell(n) + \frac{h}{8}k_1, I'_\ell(n)+\frac{k_2}{2}\right).$$

$$k_4 = hf\left(\rho_n+h, I_\ell(n)+hI'_\ell(n) + \frac{h}{2}k_3, I'_\ell(n)+k_3\right).$$

The geometrical interpretation of k values is shown in Fig. 4. All four k values represent the slopes at different points: the value k_1 is the slope at the starting point; k_4 is the slope at the right hand point whose ordinate is $I_\ell + h.I'_\ell + \frac{h}{2}k_3$; k_2 and k_3 have different slopes at the midpoint but the same ordinate $I_\ell + \frac{h}{2}I'_\ell + \frac{h}{8}k_1$.

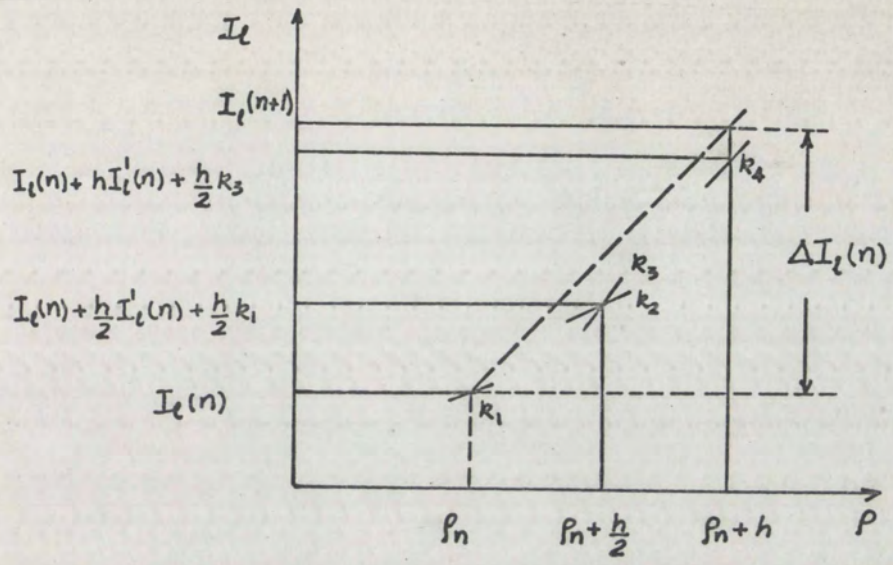

Fig. 4. Illustration of the 4 slopes used in the Runge-Kutta method.

ii) THE EULER-TAYLOR EXPANSION

The Schroedinger radial second order differential equation is

$$I'' + \frac{2}{\rho} I' + \left[m^2(\rho) - \frac{\ell(\ell+1)}{\rho^2} \right] I = 0 \quad . \tag{8}$$

The Taylor series expansion provides at $\rho_n + h$,

$$I_\ell(\rho_n + h) = I_\ell(\rho_n) + h\, I'_\ell(\rho_n) + \frac{h^2}{2} I''_\ell(\rho_n) + \cdots \tag{22}$$

$$I'_\ell(\rho_n + h) = I'_\ell(\rho_n) + h\, I''_\ell(\rho_n) + \cdots \tag{23}$$

Substitute eq.(8) into eqs. (22) and (23)

$$I_\ell(\rho_n+h) = I_\ell(\rho_n) \left\{ 1 + \frac{h^2}{2} \left[\frac{\ell(\ell+1)}{\rho_n^2} - m^2(\rho_n) \right] \right\} + h\, I'_\ell(\rho_n) \left[1 - \frac{h}{\rho} \right]. \tag{24}$$

$$I'_\ell(\rho_n+h) = \left(1-\frac{2h}{\rho_n^2}\right) I'_\ell(\rho_n) + h\left[\frac{\ell(\ell+1)}{\rho_n^2} - m^2(\rho_n)\right] I_\ell(\rho_n). \quad (25)$$

Eqs. (24) and (25) are applied step by step to calculate the I_ℓ and I'_ℓ for different values of ρ.

III. CALCULATION OF THE COEFFICIENTS A_ℓ AND C_ℓ

The constant coefficients A_ℓ and C_ℓ of eqs. (6) and (7) can be determined by requiring that the wave function and its first derivative be continuous at $r = a + \delta/k$:

$$u_{ins}(r,\theta)\Big|_{r=a+\delta/k} = u_{out}(r,\theta)\Big|_{r=a+\delta/k} , \tag{26}$$

$$\frac{d}{dr}u_{ins}(r,\theta)\Big|_{r=a+\delta/k} = \frac{d}{dr}u_{out}(r,\theta)\Big|_{r=a+\delta/k} , \tag{27}$$

$$u_{ins}(r,\theta) = \sum_{\ell=0}^{\infty} C_\ell I_\ell(kr) P_\ell(\cos\theta) . \tag{7}$$

$$u_{out}(r,\theta) = \sum_{\ell=0}^{\infty} A_\ell h_\ell^{(1)}(kr) P_\ell(\cos\theta) + \sum_{\ell=0}^{\infty} (2\ell+1) i^\ell j_\ell(kr) P_\ell(\cos\theta) . \tag{6}$$

Substitute eqs. (6) and (7) into eqs.(26) and (27)

$$A_\ell h_\ell^{(1)}(ka+\delta) - C_\ell I_\ell(ka+\delta) + (2\ell+1) i^\ell j_\ell(ka+\delta) = 0 .$$

$$A_\ell h_\ell^{(1)\prime}(ka+\delta) - C_\ell I'_\ell(ka+\delta) + (2\ell+1) i^\ell j'_\ell(ka+\delta) = 0 .$$

Solve for A_ℓ and C_ℓ :

$$A_\ell = (2\ell+1)\, i^\ell \frac{\begin{vmatrix} j_\ell(x+\delta) & I_\ell(x+\delta) \\ j'_\ell(x+\delta) & I'_\ell(x+\delta) \end{vmatrix}}{\begin{vmatrix} h_\ell^{(1)}(x+\delta) & -I_\ell(x+\delta) \\ h_\ell^{(1)\prime}(x+\delta) & -I'_\ell(x+\delta) \end{vmatrix}} .$$

$$C_\ell = -(2\ell+1)\, i^\ell \frac{\begin{vmatrix} h_\ell^{(1)}(x+\delta) & j_\ell(x+\delta) \\ h_\ell^{(1)\prime}(x+\delta) & j_\ell'(x+\delta) \end{vmatrix}}{\begin{vmatrix} h_\ell^{(1)}(x+\delta) & -I_\ell(x+\delta) \\ h_\ell^{(1)\prime}(x+\delta) & -I_\ell'(x+\delta) \end{vmatrix}} .$$

Finally,

$$A_\ell = (2\ell+1)\, i^\ell \left(\frac{j_\ell(x+\delta) I_\ell'(x+\delta) - j_\ell'(x+\delta) I_\ell(x+\delta)}{I_\ell(x+\delta) h_\ell^{(1)\prime}(x+\delta) - I_\ell'(x+\delta) h_\ell^{(1)}(x+\delta)} \right) , \qquad (28)$$

$$C_\ell = (2\ell+1)\, i^\ell \left(\frac{j_\ell(x+\delta) n_\ell'(x+\delta) - j_\ell'(x+\delta) n_\ell(x+\delta)}{I_\ell(x+\delta) h_\ell^{(1)\prime}(x+\delta) - I_\ell'(x+\delta) h_\ell^{(1)}(x+\delta)} \right) . \qquad (29)$$

The coefficients A_ℓ and C_ℓ can also be written in terms of the spherical Bessel functions and the Neumann functions, from the definition of the Hankel functions(eq. 4)
Thus,

$$A_\ell = -\frac{(2\ell+1)\, i^\ell\, F_\ell (F_\ell - iG_\ell)}{F_\ell^2 + G_\ell^2} , \qquad (30)$$

$$C_\ell = \frac{(2\ell+1)\, i^{\ell+1} \left[j_\ell(x+\delta) n_\ell'(x+\delta) - j_\ell'(x+\delta) n_\ell(x+\delta) \right] \left[F_\ell - iG_\ell \right]}{F_\ell^2 + G_\ell^2} , \qquad (31)$$

where

$$F_\ell = I_\ell(x+\delta) j_\ell'(x+\delta) - I_\ell'(x+\delta) j_\ell(x+\delta) , \qquad (32)$$

$$G_\ell = I_\ell(x+\delta) n_\ell'(x+\delta) - I'_\ell(x+\delta) n_\ell(x+\delta) . \qquad (33)$$

The probability of finding the incident particle inside the well excluding the boundary region, can be determined by integration of the intensity of the incident wave, $|u_{ins}|^2$ over the volume element $r^2\, dr\, d\Omega$:

$$PROB = 2\pi \int_0^{a-\delta/k} \int_0^{\pi} |u_{ins}|^2 r^2 \sin\theta\, d\theta\, dr. \qquad (34)$$

The integration over the polar angle θ is easily done by using the orthogonality property of the Legendre polynomials:[1,2]

$$\int_0^{\pi} d\theta \sin\theta\, P_\ell(\cos\theta) P_{\ell'}(\cos\theta) = \frac{2}{2\ell+1} \delta_{\ell\ell'}. \qquad (35)$$

where $\delta_{\ell\ell'}$ is the Kronecker delta function.
Some integral relations of spherical Bessel functions are also used:[1,2]

for $\ell \neq 0$

$$\frac{1}{k^3M^3} \int_0^{M(x-\delta)} j_\ell^2(v) v^2 dv = \frac{1}{2k^3M^3} \left| v^3 \left(j_\ell^2(v) - j_{\ell-1}(v) j_{\ell+1}(v) \right) \right|_0^{M(x-\delta)}$$

$$= \frac{[M(x-\delta)]^3}{2k^3M^3} \left[j_\ell^2(Mx-M\delta) - j_{\ell-1}(Mx-M\delta) j_{\ell+1}(Mx-M\delta) \right]. \qquad (36)$$

for $\ell = 0$

$$\frac{1}{k^3M^3} \int_0^{M(x-\delta)} j_0^2(v) v^2 dv = \frac{1}{k^3M^3} \left[\frac{1}{2} v - \frac{1}{4} \sin 2v \right]_0^{M(x-\delta)}$$

$$= \frac{1}{k^3M^3} \left[\frac{M(x-\delta)}{2} - \frac{1}{4} \sin 2M(x-\delta) \right]. \qquad (37)$$

The average probability density inside the well is obtained by dividing the total probability, PROB, over the total volume of the sphere, $4\pi a^3/3$.

The probability density after performing the integrations over θ and r is,

$$\begin{aligned} \text{PROB. DENS.} &= \frac{3}{(MX)^3}\left[\frac{MX-M\delta}{2} - \frac{1}{4}\sin 2M(X-\delta)\right] C_0^* C_0 \\ &+ \frac{3}{2}\sum_{\ell=1}^{\infty} \frac{C_\ell^* C_\ell}{2\ell+1}\left(1-\frac{\delta}{X}\right)^3 \left[j_\ell^2(MX-M\delta) - j_{\ell-1}(MX-M\delta) j_{\ell+1}(MX-M\delta)\right] . \end{aligned} \tag{38}$$

The asymptotic form of the outside scattered wave can be written in terms of the directional dependence, $f(\theta)$[1,2] of the amplitude.

$$u_{os}(\infty, \theta) = \frac{f(\theta)\, e^{ikr}}{r} , \tag{39}$$

where

$$f(\theta) = \frac{1}{k}\sum_{\ell=0}^{\infty} A_\ell\, e^{-i(\ell+1)\frac{\pi}{2}} P_\ell(\cos\theta) . \tag{40}$$

The differential cross section is given by[1,2]

$$\frac{d\sigma}{d\Omega} = \left|f(\theta)\right|^2 . \tag{41}$$

Substitution of eq.(40) into eq.(41) gives,

$$k^2 \frac{d\sigma}{d\Omega} = \left|\sum_{\ell=0}^{\infty} A_\ell\, e^{-i(\ell+1)\frac{\pi}{2}} P_\ell(\cos\theta)\right|^2 . \tag{42}$$

We obtain the total scattering cross section by integration of the differential cross section over the solid angle $d\sigma$:

$$k^2 \sigma = 4\pi \sum \frac{|A_l|^2}{2l+1} . \qquad (43)$$

IV. FORTRAN PROGRAM

The use of a computer is required to investigate the effect of a narrow surface transition region on the scattering process at high values of ℓ of the Schroedinger three dimensional square well potential.

Some samples of the results were obtained with the 360 IBM Model 40 computer, which provides 16 significant figures running with double precision variables.

The probability density, total cross section, and differential cross section are real variables since they represent physical observables.

In order to calculate the differential cross section it is necessary to rewrite f(θ) by substitution of eq.(30) into eq. (40):

$$f(\theta)=\frac{1}{k}\left[\sum_{\ell=0}^{L}\frac{(2\ell+1)\,F_\ell G_\ell P_\ell(\cos\theta)}{F_\ell^2+G_\ell^2}+\; i\cdot\sum_{\ell=0}^{L}\frac{(2\ell+1)\,F_\ell^2 P_\ell(\cos\theta)}{F_\ell^2+G_\ell^2}\right]e^{-i(\ell+1)\frac{\pi}{2}}. \qquad (44)$$

Replace eq.(44) into eq. (41):

$$k^2\frac{d\sigma}{d\Omega}=\left[\sum_{\ell=0}^{L}\frac{(2\ell+1)\,F_\ell G_\ell P_\ell(\cos\theta)}{F_\ell^2+G_\ell^2}\right]^2+\left[\sum_{\ell=0}^{L}\frac{(2\ell+1)\,F_\ell^2 P_\ell(\cos\theta)}{F_\ell^2+G_\ell^2}\right]^2. \qquad (45)$$

A FORTRAN program was written to calculate the probability density, the differential and total cross section at high

values of L. The recursion relations were used to generate a set of spherical Bessel and Neumann functions, and also for their derivatives:[1]

$$f_\ell(z) = \frac{2\ell-1}{z} f_{\ell-1}(z) - f_{\ell-2}(z) . \qquad (46)$$

$$\frac{d}{dz} f_\ell(z) = f_{\ell-1}(z) - \frac{\ell+1}{z} f_\ell(z) . \qquad (47)$$

where $f_\ell(z)$ holds for Bessel and Neumann functions.
We start with:

$$j_o(X) = \sin X / X ,$$

$$j_1(X) = (\sin X / X^2) - \cos X / X ,$$

$$n_o(X) = - \cos X / X ,$$

$$n_1(X) = -(\cos X / X^2) - \sin X / X .$$

The Legendre polynomials are generated by using the recursion relations:[1]

$$P_\ell(z) = \frac{1}{\ell} \left[(2\ell-1) z P_{\ell-1}(z) - (\ell-1) P_{\ell-2}(z) \right] .$$

The starting functions are:

$$P_o(\cos\theta) = 1.$$

$$P_1(\cos\theta) = \cos\theta .$$

The number of terms that will include in our series come to be slightly greater than the size parameter[7,9] since the terms with ℓ much greater than X would completely

miss the spherical potential and should not be expected to contribute to the other terms of the series. This can be seen in terms of the partial wave analysis in quantum theory[9]: the nth term is associated with an orbital angular momentum, $nh/2\pi$, which corresponds classically to a particle with momentum h/λ at an impact parameter of $n\lambda/2\pi$. Thus the convergence of the series shortly after n exceeds X results from the fact that the incident particle does not pass through the sphere any longer.

For most of the calculations 30 terms past the argument of the Bessel, Neumann functions and the Legendre polynomials were included in our analysis to show this convergence.

A FORTRAN program (appendix) allows the choice of any initial and final value for the size parameter X, and for the azimuthal angle θ, with arbitrary increments of ΔX and $\Delta\theta$. Other parameters are the number of divisions (div) and δ, the half-width of the transition region.

Figure 5 shows a flow chart of this program.

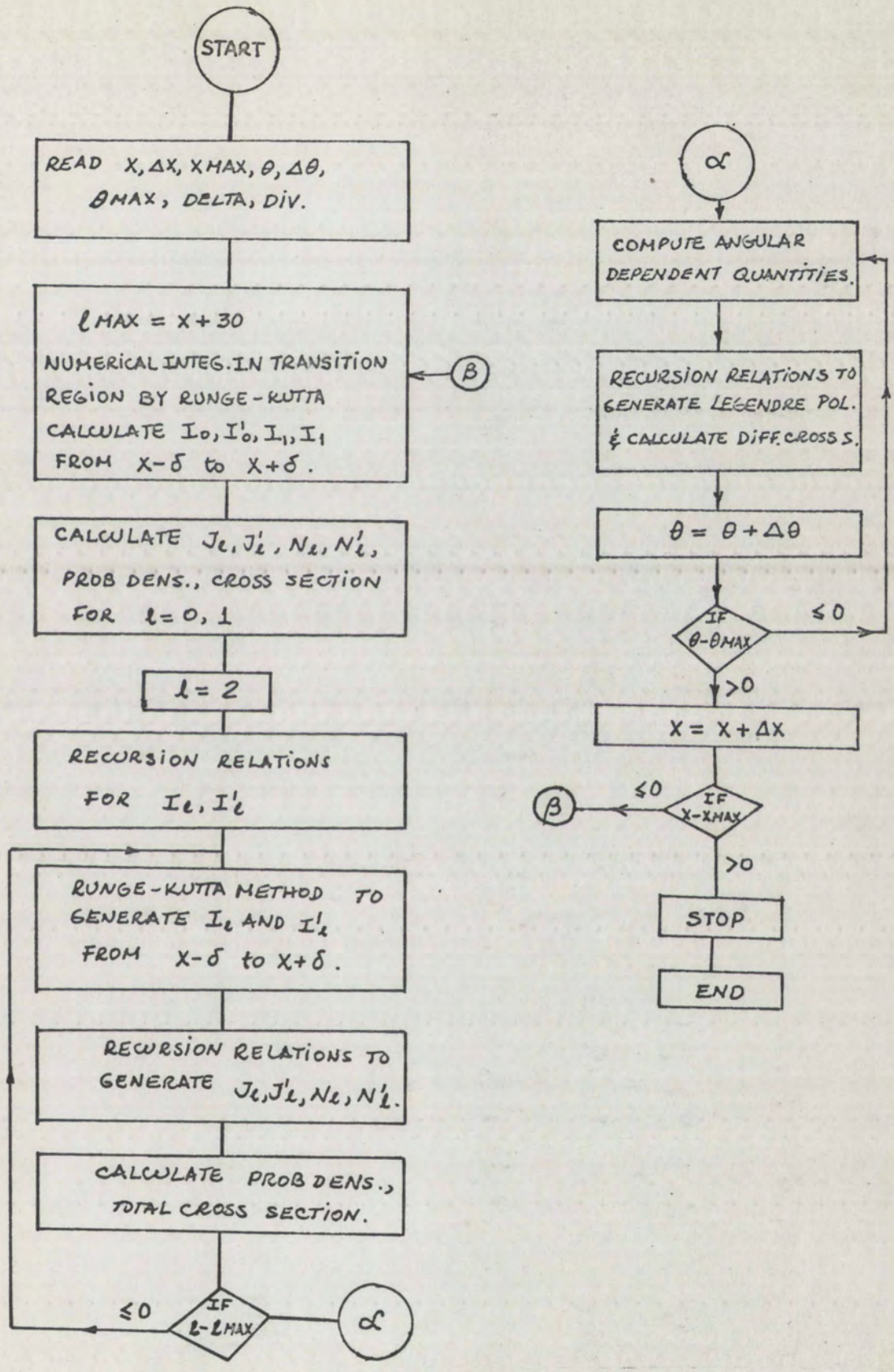

Figure 5. Flow chart of the FORTRAN program.

V. RESULTS

The existence of four different resonances for size parameter near 200 was reported before[7] for the special case of a perfect square well (no transition region). The period of these resonances was found[7] to be about 0.81 in the size parameter X.

Fig. 6 is a plot of the radial probability distribution for $\delta=0$, $X=200.7469$ and shows that a number of fluctuations arises in the region $0.75\,a \leq r \leq a$, the number of these oscillations determining the "type". We call this example a type 8 resonance because of the 8 distinct peaks. Similarly, the other resonances are called type 6, 7, 9 resonances, in correspondence to the number of peaks that they have in the region $0.75\,a \leq r \leq a$ in the plot of the radial probability distribution vs r (size parameter fixed and calculated at the peak value of the resonance). A comparison of these different resonances is shown in table 1, page 26.

In this paper, a study of how the peak height (probability density at maximum) and the width of the resonances behave as δ increases is made.

The width of the resonances was calculated under the assumption that they have a Lorentzian line shape of the form:

$$f(x') = \frac{H}{1 + (x'-x_0)^2/\sigma^2} ,$$

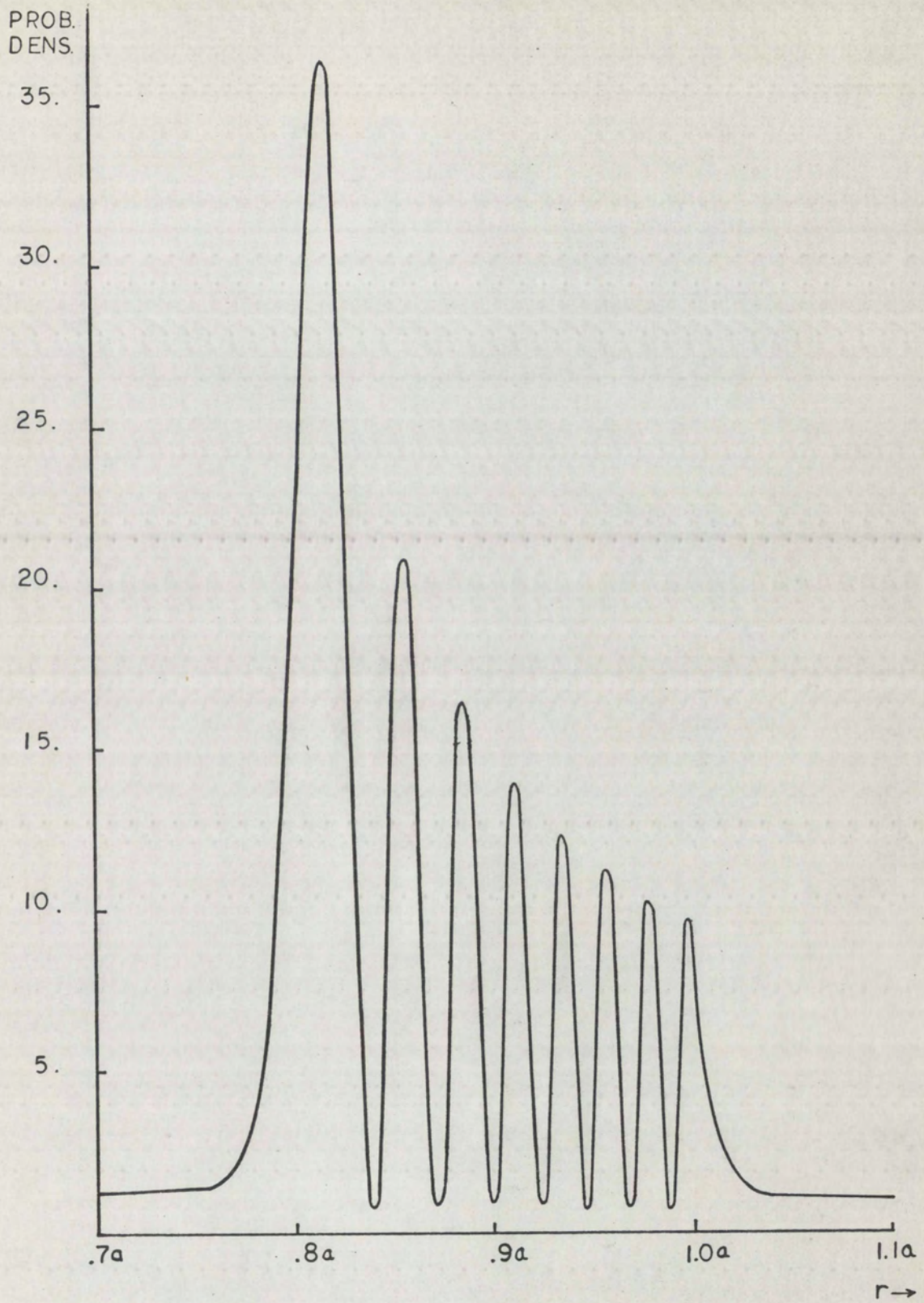

Fig. 6 : X_0=200.7469, δ=0 , 200 div.

where 2σ (FWHM), H , and X_o represent the full width at half maximum, the height of the peak and the position at the peak respectively (Fig. 7).

We concentrated on the type 8 resonance throughout this paper since the other resonances have a quite similar behavior.

A sample of the results obtained for the type 8 resonance is shown in Fig. 7, which compares the Runge-Kutta method with the Euler-Taylor expansion of the probability density vs the size parameter X, for $\delta = 10^{-4}$, $\Delta X = 5.10^{-4}$ and 200 div.

Fig. 8 is a plot of the growth of the series for the type 8 resonance yielding the probability density at $\delta = 10^{-4}$, X = 200.7165, and 200 div, with respect to the highest term of the angular momentum using in computing it. This graph may be interpreted in terms of the partial wave analysis in quantum theory[9] as indicated in page 19. The examination of the growth curve shows that there is a strong contribution near the surface of the well; the existence of surface resonances are postulated, and it appears that they are of great importance in the scattering process.

Fig. 9 is a plot of the total cross section vs the number of divisions in half of the transition region. The total cross section variable was chosen since it remains quite constant as the number of divisions is increased.

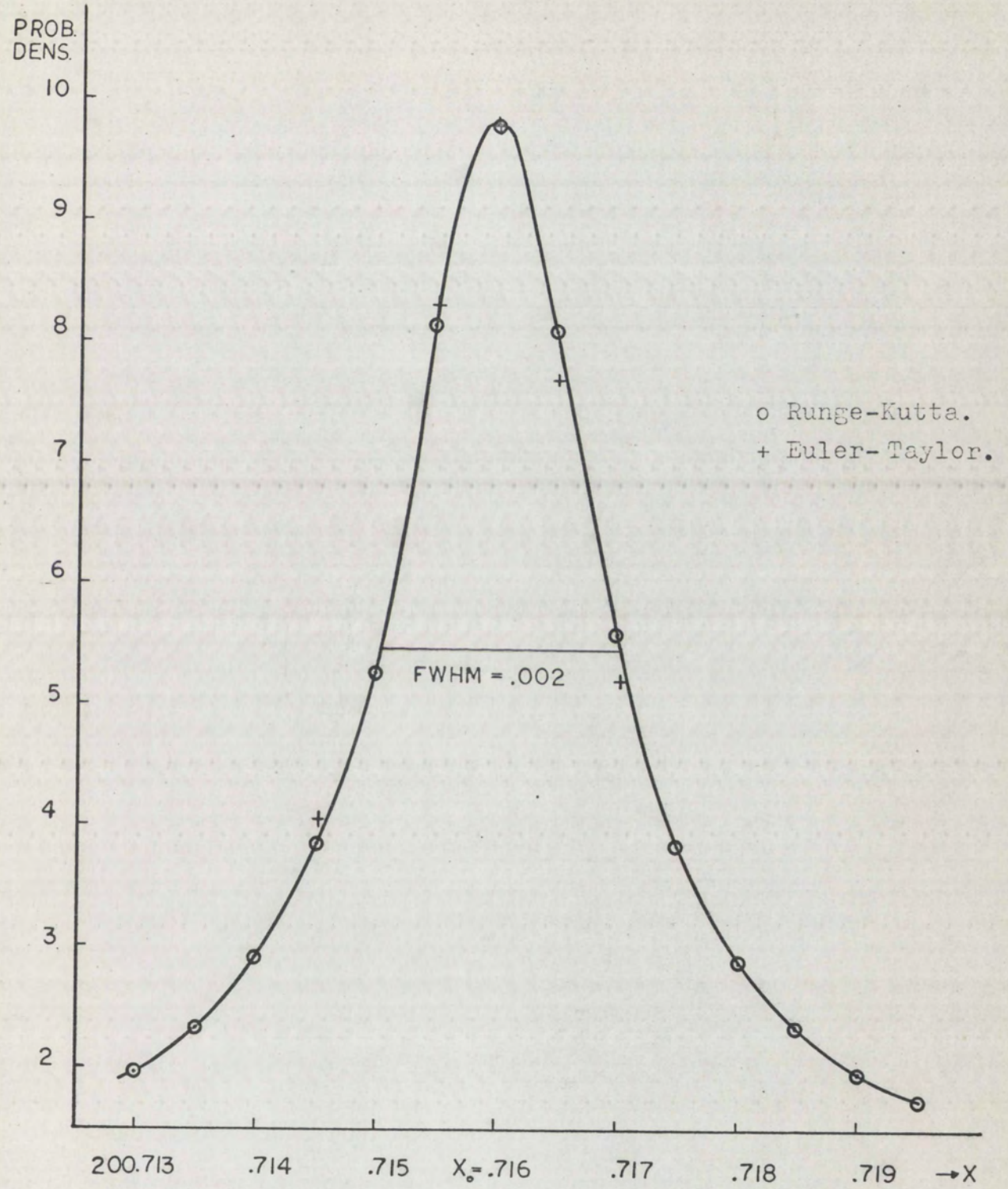

Fig. 7. Probability density vs X, for $\delta = 10^{-4}$, X= 0.0005, 200 div.

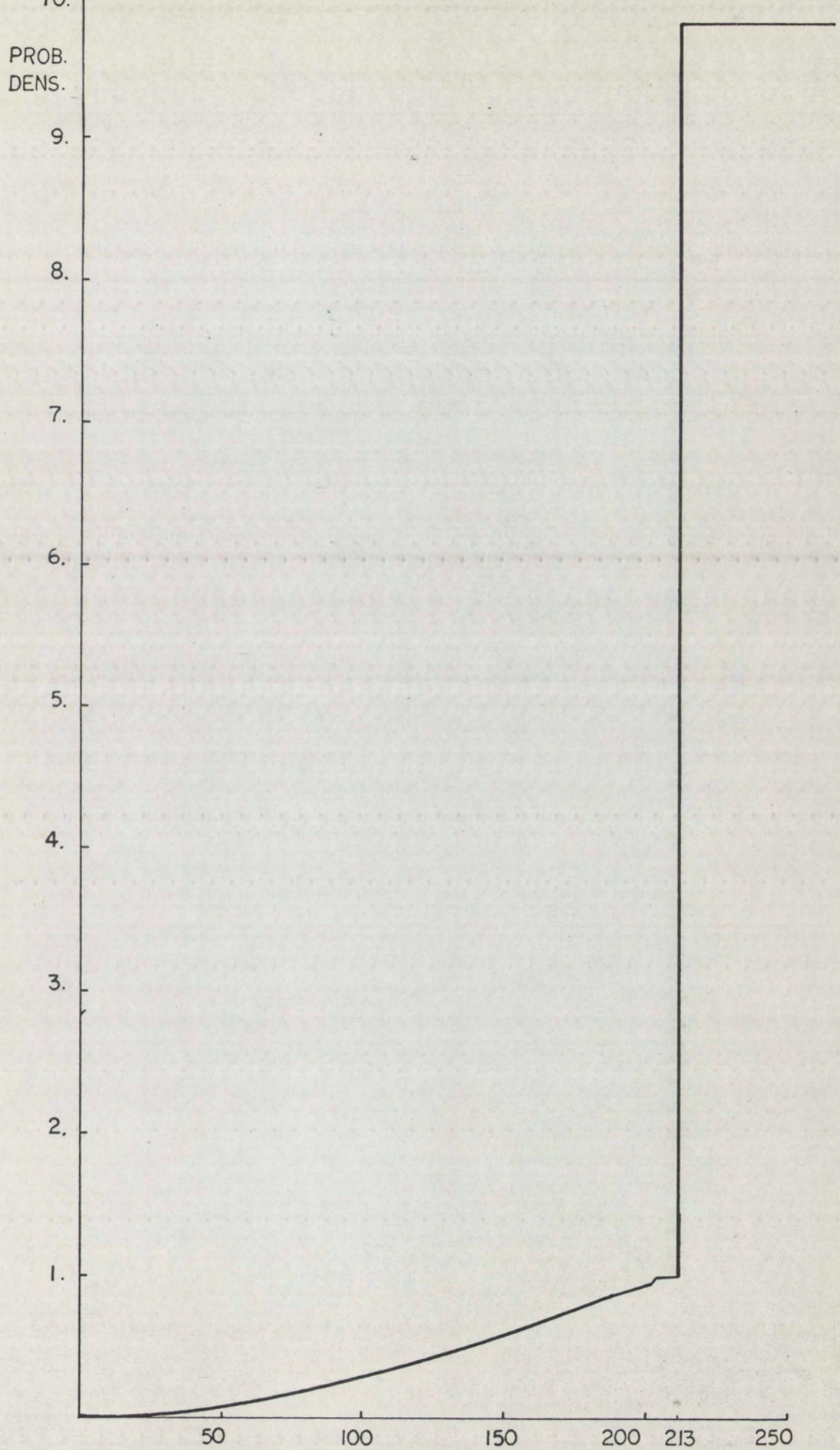

Fig. 8.- Growth of series(Type 8)

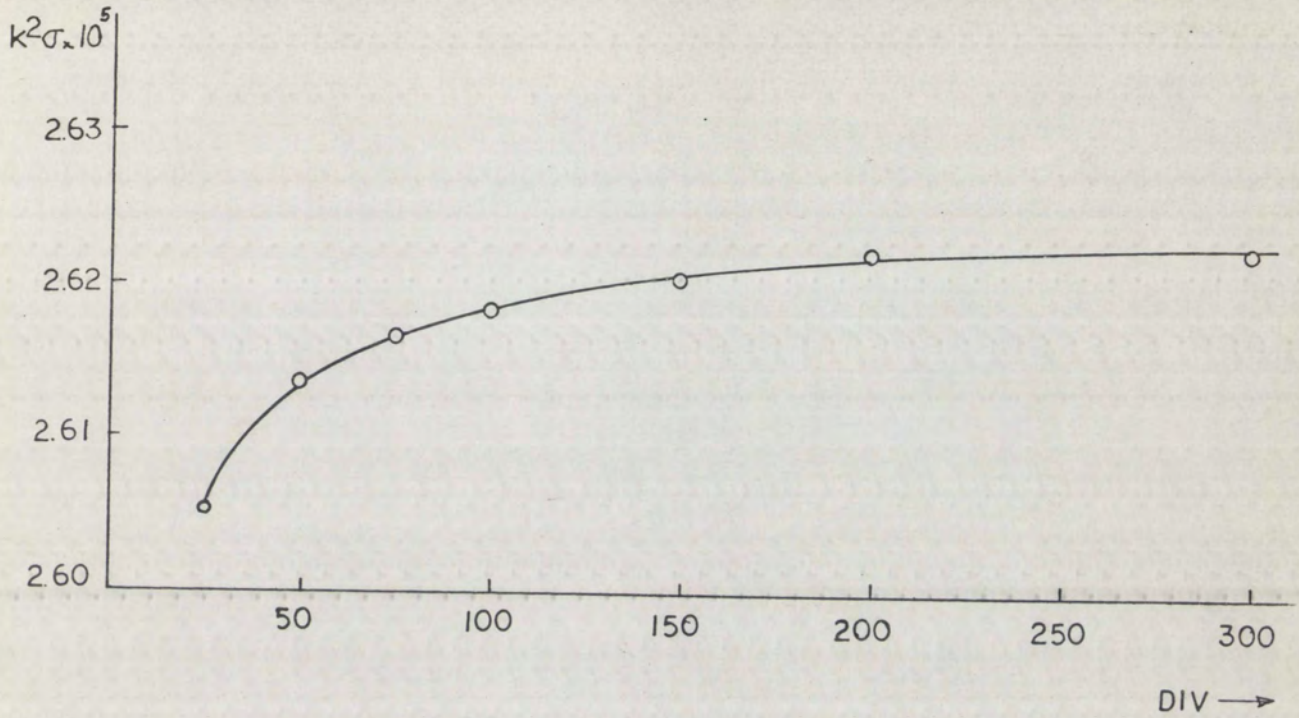

Fig. 9. Plot of cross section times k^2 vs the number of divisions in half of the transition region.

	MAXIMUM PROB DENS.	X_o	FWHM	ℓ_{growth}
TYPE 6	1.3092×10^5	200.776799	8×10^7	223
TYPE 7	314.6975	200.855270	4.3×10^5	218
TYPE 8	9.8136	200.7165	2×10^3	213
TYPE 9	1.567281	200.379	0.0296	208

Table 1. Comparison of the four different resonances for $\delta = 10^{-4}$, 200 div.

A value of 200 div. was selected for results quoted throughout this paper, in order that our results could be given reasonably accurately (less than one percent of error).

Table 1 compares the different values for the probability density, width and position at the peak obtained for the four kinds of resonances. The last column of the table gives the term for which the growth of the curve converges.

The phenomenon of resonances can be explained as follows: If one thinks of a wave traveling around and around the spherical surface, one can see that the longer the attenuation length, the sharper the resonance will be. A long attenuation length means that the particle will be around the surface a long time before it is scattered. This effect is analogous to the sharpness of the interference pattern for the Fabry-Perot interferometer: the longer (more reflections) a monochromatic light beam stays inside the system, the sharper the line will be.

Fig. 10 is a plot of the position at the peak, X_o, vs the parameter δ. The region that we have investigated is very small compared to the magnitude of the size parameter X ; a linear dependence of X_o vs δ was found. That X_o decreases as δ increases means that the effective diameter of the well is increasing as the width of the transition zone increases.

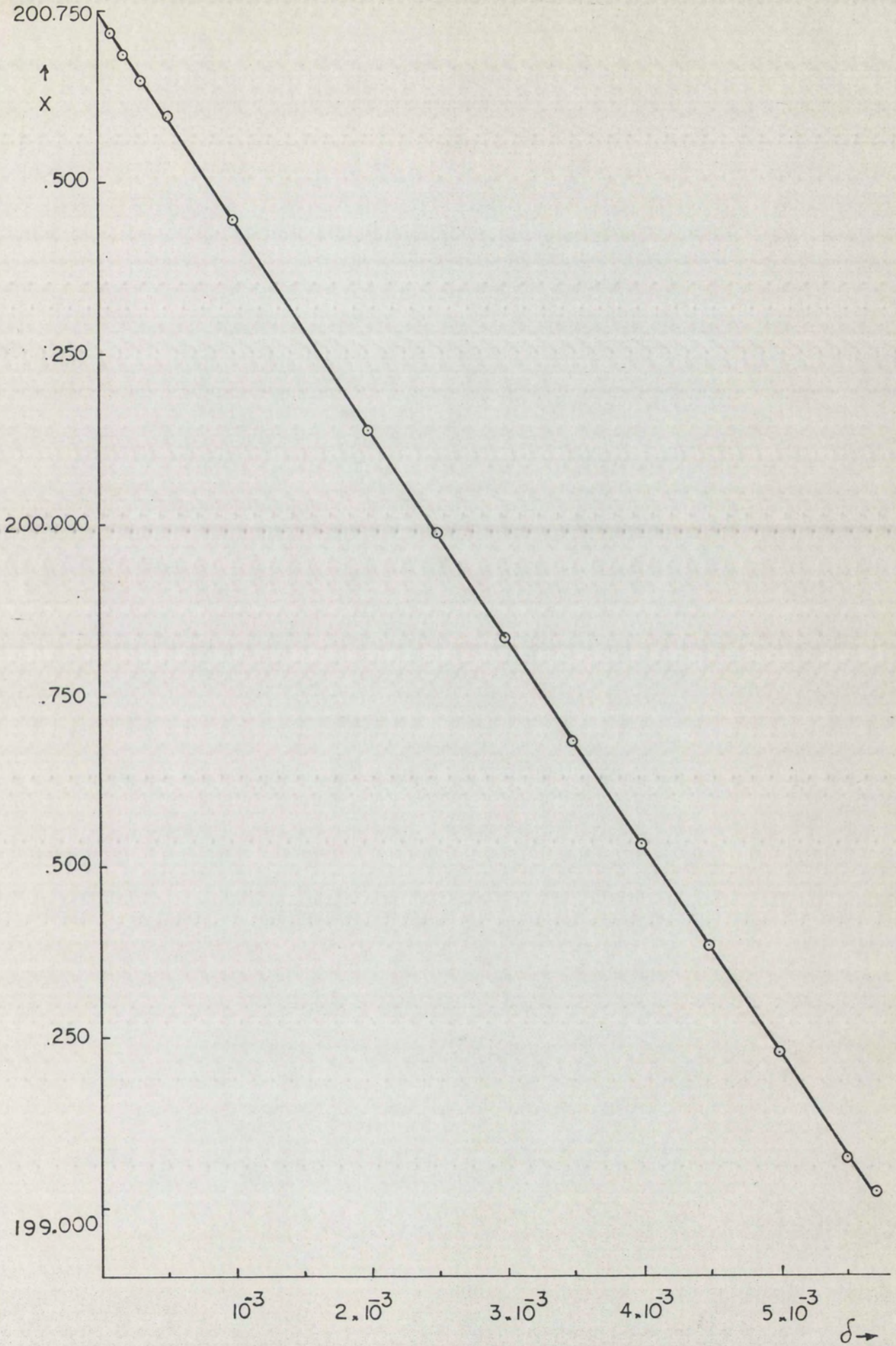
200.750
X
.500
.250
200.000
.750
.500
.250
199.000
10^{-3}
2.10^{-3}
3.10^{-3}
4.10^{-3}
5.10^{-3}
δ

Fig 10.

Fig. 11 is a plot of the full width at half maximum vs the half-width of the transition region δ. It shows that the width decreases as δ becomes larger.
The dependence of the full width on δ is not linear as is the dependence of X_o on δ. We made $\Delta X \sim 4.10^{-4}$ for the plot of Fig. 11.

Fig. 12 is a plot of the peak probability density vs δ, the half-width of the transition region. The region investigated ($\delta \leq 5.10^{-3}$) shows that there is a linear dependence of the peak probability density vs the half-width of the transition region, δ.

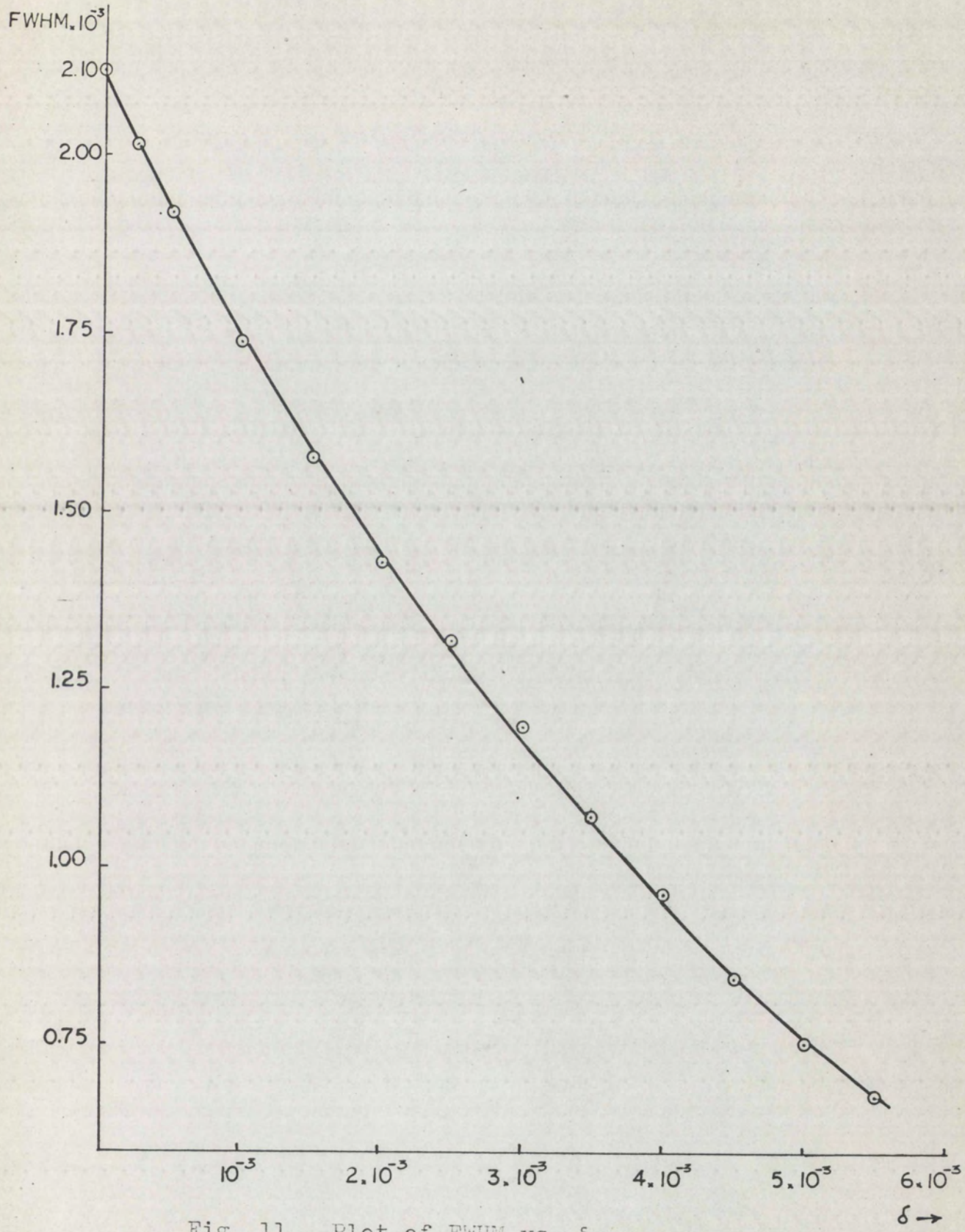

Fig. 11. Plot of FWHM vs. δ

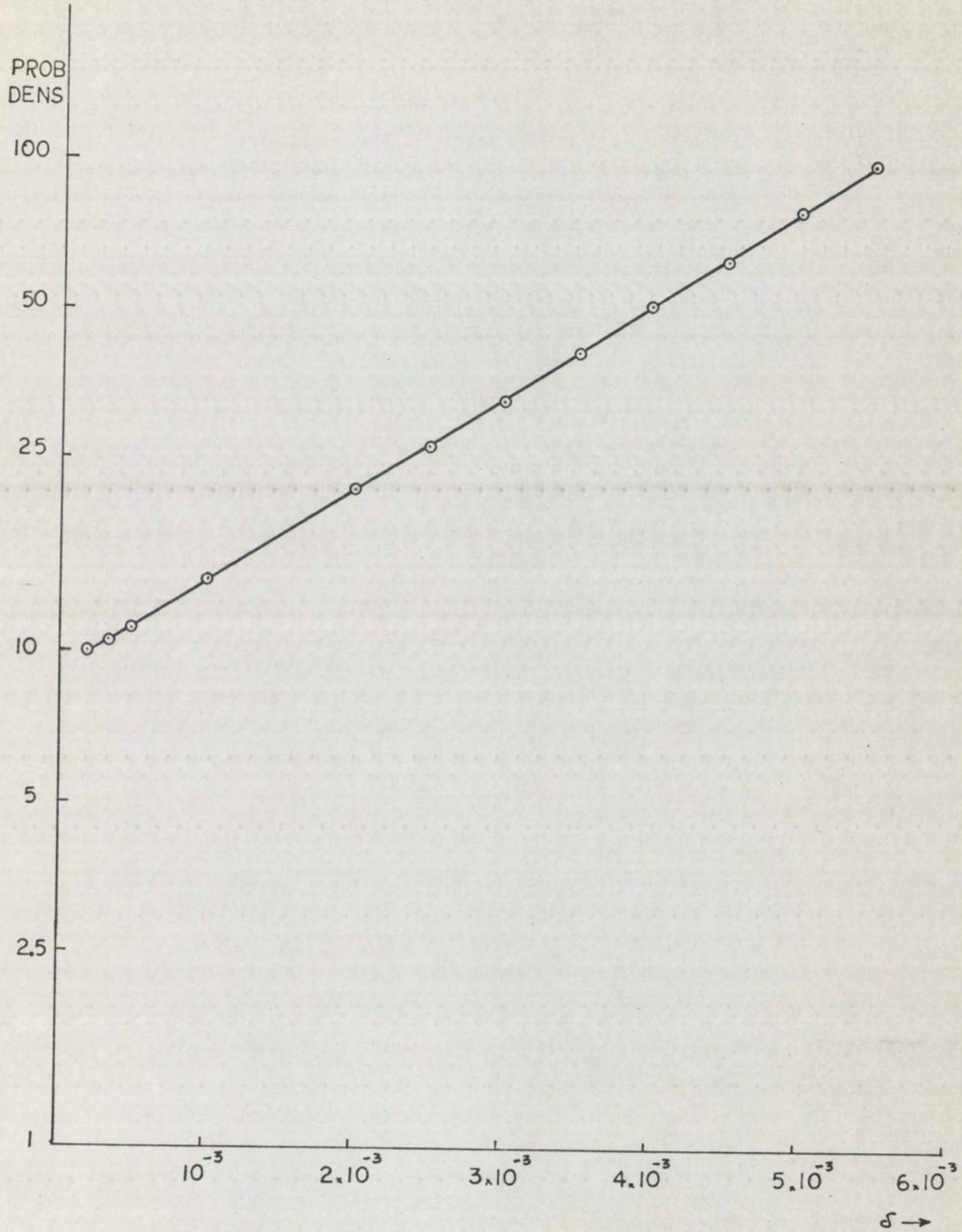

Figure 12. Plot of peak prob. dens. vs. δ
Vertical axes in logarithm scale.

VI. DISCUSSION

In this paper we examined the regions of the size parameter near resonances, which play an important role in the backscattering process. These surface resonances are produced with the help of surface waves, which arise when energy strikes the interface between two dielectrics from the more dense medium at the critical angle for total reflection,[10] or at a greater angle. The surface wave would have to travel around the sphere many times to get the necessary sharpness of the resonances.

A transition zone introduced between the interface of the two dielectrics would increase the surface wave intensity so that more energy gets to the surface because of a better "impedance matching" than for the case of having no transition zone between the dielectrics. This is a possible explanation of Fig. 12 (the probability density increases as δ does).

VII. CONCLUSIONS

We have examined theoretically the surface resonances excited by a monochromatic beam of particles on a spherical well (analogous to the scattering of light by water droplets) with a very small transition region.

The main features are:

1. Thede's results were verified and the precision in certain numbers was improved.
2. The resonances are enhanced by introducing a transition region.
3. As the half-width of the transition region, δ, increases:
   a) The size parameter at resonance, X_o, decreases.
   b) The full-width at half maximum decreases (exponentially?, asymptotically?).
   c) The probability density increases linearly with δ.

APPENDIX

FORTRAN PROGRAM

```
      C     INTERACTION OF A PLANE WAVE WITH A
      C     THREE-DIMENSIONALSQUARE WELL WITH A TRANSITION
      C     REGION. COMPUTATION OF THE DIFFERENTIAL(SIGM)
      C     AND TOTAL CROSS SECTION AND AVERAGE
      C     PROBABILITY DENSITY(PROB)
0001        DIMENSION SIE(2000), SIF(2000), CSC(2000),
           1PE(50), IM(50),SIGM(500)
0002        INTEGER R,P
0003        R=5
0004        P=6
0005        DOUBLE PRECISION JXD0,JXD1,JXDP0,JXDP1,NXDP0,
           1NXDP1,XD,DELTA,X,RE,MRE,NXD0,NXD1,IX0,IXP0,
           2IX1,IXP1,JMRE0,JMRE1,IXL,IXPL,JXDL,NXDL,
           3JXDPL,NXDPL,JMREL,JMRELL,MXD,
           4THTA,PI,DX,XMAX,A,C,D,F,AJ,PE,IM, M,MX,Z, P1,
           5PL,SIE,SIF,MQ ,X0,PROB,SIGM,P0,SUM
0006        DOUBLE PRECISION   Q,MW,MD,AW,BW,CW,G0,G1,DUM,
           1K10,G0H,G0HH,K20,K30,MWHH,K40,G1H,G1HH,K11,K21,
           2K31,K41,H,U,DIV,CJ,CSC ,MWH,CROS
           3,DTHT,THTM,THT0
0007     20 READ(R,1001)X,DX,XMAX,THTA,DTHT,THTM,M,X0
0008   1001 FORMAT(3F9.5,3F8.2,F8.4,F8.3)
0009        READ(R,10)DELTA,DIV
0010     10 FORMAT(F12.9,F12.6)
0011        WRITE(P,90)X,DX,XMAX,THTA,DTHT,THTM,M,X0
0012     90 FORMAT(3H1X=,F9.3,4H DX=,F5.3,6H XMAX=,F9.3,
           16H THTA=,F6.1,6H DTHT=,F5.2,6H THTM=,F5.1,
           23H M=,F7.4,4H X0=,F9.3)
0013        WRITE(P,91) DELTA,DIV
0014     91 FORMAT(7H DELTA=,E13.6,5H DIV=,E12.6)
0015     50 LMAX=X+ 30
0016        MX=M*X
0017        XD=X+DELTA
0018        MXD=M*XD
      C     ROUTINE TO INTEGRATE NUMERICALLY THROUGH OHE
      C     TRANSITION ZONE USING THE RUNGE-KUTTA METHOD
      C     CALCULATE PARAMETERS OF A CUBIC TO REPRESENT THE
      C     INDEX OF REFRACTION IN THE TRANSITION ZONE
      C     2*DELTA IS THE WIDTH OF THE TRANSITION ZONE
0019        H=DELTA/DIV
0020        AW=(M+1.0)/2.0
0021        BW=-3.0*(M-1.0)/(4.0*DELTA)
0022        CW=-BW/(3.0*DELTA**2)
0023        Q=X-DELTA
0024        D=-DELTA
0025        MD=M*D
0026        MQ=M*Q
0027        IX0=DSIN(MQ)/MQ
```

```
0028                IX1=DSIN(MQ)/MQ**2-DCOS(MQ)/MQ
0029                IXP0=M*(DCOS(MQ)/MQ-DSIN(MQ)/MQ**2)
0030                IXP1=(IX0-2.0*IX1/MQ)*M
0031                N=0
0032                U=X+DELTA
0033          100   MW   =AW+BW*D +CW*D**3
0034                Q=N*H+X-DELTA
0035                D=N*H-DELTA
0036                G0     = -MW    **2
0037                K10=H*G0*IX0-2.0*H*IXP0/Q
0038                G1     =G0     +2.0/ Q**2
0039                K11=H*G1*IX1-2.0*H*IXP1/Q
0040                D=D+H/2.0
0041                MWH  =AW+BW*D +CW*D**3
0042                G0H  =-MWH**2
0043                Q=Q+H/2.0
0044                K20=H*G0H*(IX0+H*IXP0/2.0+H*K10/8.0)-
                   12.0*H*(IXP0+K10/2.0)/ Q
0045                K30=H*G0H*(IX0+H*IXP0/2.0+H*K10/8.0)-
                   12.0*H*(IXP0+K20/2.0)/ Q
0046                G1H  =G0H   +2.0/ Q**2
0047                K21=H*G1H*(IX1+H*IXP1/2.0+H*K11/8.0)-
                   12.0*(IXP1+K11/2.0)*H/Q
0048                K31=H*G1H*(IX1+H*IXP1/2.0+H*K11/8.0)-
                   12.0*(IXP1+K21/2.0)*H/Q
0049                D=D+H/2.0
0050                Q=Q+H/2.0
0051                MWHH=AW+BW*D+CW*D**3
0052                G0HH = -MWHH **2
0053                K40=H*G0HH*(IX0+H*IXP0+H*K30/2.0)-
                   12.0*H*(IXP0+K30)/ Q
0054                IX0=IX0+H*(IXP0+(K10+K20+K30)/6.0)
0055                IXP0=IXP0+(K10+2.0*K20+2.0*K30+K40)/6.0
0056                G1HH   =G0HH   +2.0/ Q**2
0057                K41=H*G1HH*(IX1+H*IXP1+H*K31/2.0)-
                   12.0*H*(IXP1+K31)/Q
0058                IX1=IX1+H*(IXP1+(K11+K21+K31)/6.0)
0059                IXP1=IXP1+(K11+2.0*K21+2.0*K31+K41)/6.0
0060                N=N+1
0061                IF(Q-U) 100,110,110
0062          110   CONTINUE
0063                RE=X-DELTA
0064                MRE=M*RE
0065                JMRE0=DSIN(MRE)/MRE
0066                JMRE1=DSIN(MRE)/MRE**2-DCOS(MRE)/MRE
0067                JXD0=DSIN(XD)/XD
0068                JXD1=DSIN(XD)/XD**2-DCOS(XD)/XD
0069                NXD0=-DCOS(XD)/XD
```

```
0070                NXD1=-DCOS(XD)/XD**2-DSIN(XD)/XD
0071                JXDP0=DCOS(XD)/XD-DSIN(XD)/XD**2
0072                JXDP1=JXD0-2.0*JXD1/XD
0073                NXDP0=DSIN(XD)/XD+DCOS(XD)/XD**2
0074                NXDP1=NXD0-2.0*NXD1/XD
0075                A=IX0*JXDP0-IXP0*JXD0
0076                C=IX0*NXDP0-IXP0*NXD0
0077                CSC(1)=(JXD0*NXDP0-JXDP0*NXD0)**2/(A*A+C*C)
0078                SIE(1)=A*C/(A*A+C*C)
0079                SIF(1)=A*A/(A*A+C*C)
0080                PROB=((MX-M*DELTA)/2.0-DSIN(2*M*(X-DELTA))/4.)*
                   13.*CSC(1)/MX**3
0081                D=IX1*JXDP1-IXP1*JXD1
0082                F=IX1*NXDP1-IXP1*NXD1
0083                CSC(2)=9*(JXD1*NXDP1-JXDP1*NXD1)**2/(D*D+F*F)
0084                SIE(2)=D*F/(D*D+F*F)
0085                SIF(2)=D*D/(D*D+F*F)
0086                JMREL=3*JMRE1/MRE-JMRE0
0087                PROB=PROB+ ((1.-DELTA/X)**3)*CSC(2)*
                   1(JMRE1**2-JMRE0*JMREL)/2.0
0088                SUM=A*A/(A*A+C*C)
0089                SUM=SUM+3.*D*D/(D*D+F*F)
0090                L=2
0091          440   Q=X-DELTA
0092                IXL=(2*L-1)*IX1/MQ - IX0
0093                IXPL=(IX1 - (L+1)*IXL/MQ)*M
0094                N=0
                C       RUNGE-KUTTA METHOD TO GENERATE THE SPECIAL
                C       BESSEL FUNCTIONS OF HIGHER ANGULAR MOMENTUM.
0095          400   Q=N*H +X-DELTA
0096                D=N*H-DELTA
0097                MW=AW+BW*D+CW*D**3
0098                G0=-MW**2
0099                G1    =G0     +L*(L+1)/Q**2
0100                K11=H*G1*IXL - 2.0*H*IXPL/Q
0101                D=D+H/2.0
0102                Q=Q+H/2.0
0103                MWH=AW+BW*D+CW*D**3
0104                G0H=-MWH**2
0105                G1H   =G0H    +L*(L+1)/Q**2
0106                K21=H*G1H*(IXL+H*IXPL/2.0+H*K11/8.0) -
                   12.0*H*(IXPL+K11/2.0)/Q
0107                K31=H*G1H*(IXL+H*IXPL/2.0+H*K11/8.0) -
                   12.0*H*(IXPL+K21/2.0)/Q
0108                D=D+H/2.0
0109                Q=Q+H/2.0
0110                MWHH=AW+BW*D +CW*D**3
0111                G0HH=-MWHH**2
```

```
0112                    G1HH =G0HH   +L*(L+1)/Q**2
0113                    K41=H*G1HH*(IXL+H*IXPL+H*K31/2.0)-
                       12.0*H*(IXPL+K31)/Q
0114                    IXL=IXL + H*(IXPL+(K11+K21+K31)/6.0)
0115                    IXPL=IXPL + (K11 +2.0*(K21+K31) +K41)/6.0
0116                    N=N+1
0117                    IF(Q-U) 400,410,410
0118                410 CONTINUE
0119                    JXDL=(2*L-1)*JXD1/XD-JXD0
0120                    NXDL=(2*L-1)*NXD1/XD-NXD0
0121                    JXDPL=JXD1-(L+1)*JXDL/XD
0122                    NXDPL=NXD1-(L+1)*NXDL/XD
0123                    JMREL=(2*L-1)*JMRE1/MRE-JMRE0
0124                    JMRELL=(2*L+1)*JMREL/MRE-JMRE1
0125                    J=L+1
0126                    AJ=IXL*JXDPL-IXPL*JXDL
0127                    CJ=IXL*NXDPL-IXPL*NXDL
0128                    CSC(J)=((2*L+1)*(JXDL*NXDPL-JXDPL*NXDL))**2/
                       1(AJ*AJ+CJ*CJ)
0129                    SIE(J)=AJ*CJ/(AJ*AJ+CJ*CJ)
0130                    SIF(J)=AJ*AJ/(AJ*AJ+CJ*CJ)
0131                    PROB=PROB+((1.-DELTA/X)**3)*CSC(J)*3.0*
                       1(JMREL**2-JMRE1*JMRELL)/(4.0*L+2.0)
0132                    SUM=SUM+(2*L+1)*AJ*AJ/(AJ*AJ+CJ*CJ)
0133                    DUM=4*3.1415927*SUM
0134                    WRITE(P,800) L,PROB,DUM,X
0135                800 FORMAT(I6,F12.6,D15.6,F12.6)
0136                    L=L+1
0137                    IF (L-LMAX) 420,420,430
0138                420 JXD0=JXD1
0139                    JXD1=JXDL
0140                    NXD0=NXD1
0141                    NXD1=NXDL
0142                    JMRE0=JMRE1
0143                    JMRE1=JMREL
0144                    JMREL=JMRELL
0145                    IX0=IX1
0146                    IX1=IXL
0147                    GO TO 440
0148                430 PI=3.1415927
0149                    CROS=4*PI*SUM
                    C   NOW COMPUTE ANGULAR DEPENDENT QUANTITIES
0150                    THTO=THTA
0151                    K=1
0152                350 L=1
0153                    P0=1
0154                    Z=DCOS(THTA*PI/180.)
0155                    P1=Z
```

```
0156                PE(K)=SIE(1)
0157                IM(K)=SIF(1)
0158          330   J=L+1
0159                PE(K)=PE(K)+(2*L+1)*SIE(J)*P1
0160                IM(K)=IM(K)+(2*L+1)*SIF(J)*P1
0161                SIGM(K)=PE(K)**2+IM(K)**2
0162                WRITE(P,850) L,(SIGM(K),K=1,7),CROS
0163          850   FORMAT(I6,7D12.4,D12.4)
0164                L=L+1
0165                PL=((2*L-1)*Z*P1-(L-1)*P0)/L
0166                P0=P1
0167                P1=PL
0168                IF (L-LMAX) 330,330,340
0169          340   K=K+1
0170                THTA=THTA+DTHT
0171                IF(THTA-THTM) 350,350,360
0172          360 CONTINUE
0173                THTA=THTO
0174                END
```

BIBLIOGRAPHY

1. Leonard I. Schiff, Quantum Mechanics (New York: Mc Graw Hill Book Co., 1955), pp 76,101,102,104,78
2. Eugen Merzbacher, Quantum Mechanics (New York: John Wiley and Sons, Inc., 1966), pp 207, 179,218,219,220,221.
3. Albert Messiah, Quantum Mechanics, Vol 1 (New York: John Wiley and Sons, Inc., 1965) p.386.
4. Handbook of Mathematical Functions (1964), National Bureau of Standards, p.334.
5. Shan S. Kuo, Numerical Methods and Computers (Addison-wesley, Reading, Massachusetts,1965) pp 108,109.
6. J. B. Scarborough, Numerical Mathematical Analysis (The Johns Hopkins Press, 1961) p.358.
7. Robert R. Thede, High Frequency Scattering from a Schroedinger square well (Master Thesis, University of New Mexico, 1967).
8. Daniel Mc Craken, Fortran IV (John Wiley and Sons,Inc., 1965).
9. H.C. Bryant and A.J. Cox, J. Opt. Soc. Am. 56, 1529 (1966).
10. T.S. Fahlen and H.C. Bryant, Optical Backscattering from Single Water Droplets - to be published.